

Support Information

***In situ* mineralized PLGA/zwitterionic hydrogel composites scaffolds enable high-efficiency rhBMP-2 release for critical-sized bone healing**

Peiming Liu^{a, d} [§], Tianyi Bao^c, [§], Lian Sun^c, [§], Zeyi Wang^a, Jin Sun^a, Wan Peng^a, Donglin Gan^a, Guoyong Yin^c, Pingsheng Liu^{a,*}, Wei-Bing Zhang^{b, c} ^{*}, Jian Shen^{a,e,*}

^a Jiangsu Collaborative Innovation Center of Biomedical Functional Materials, Jiangsu Key Laboratory of Bio-functional Materials, School of Chemistry and Materials Science, Nanjing Normal University, Nanjing 210023, P. R. China

^b Department of Stomatology, Dushu Lake Hospital Affiliated to Soochow University, Medical Center of Soochow University

^c Department of Orthopedics, Jiangsu Key Laboratory of Oral Diseases, Nanjing Medical University, Nanjing 210029, P. R. China

^d Changzhou Institute of Materia Medica Co., Ltd., Changzhou, Jiangsu 213000, China

^e Jiangsu Engineering Research Center of Interfacial Chemistry, Nanjing University, Nanjing 210093, P. R. China

[§]These authors contributed equally to this work.

*Corresponding authors. Email: liups@njnu.edu.cn (P. L.); wbzhang@suda.edu.cn (W. Z.) shenjian@nju.edu.cn (J. S.)

1. Preparation of m-PLGA/PSBMA scaffolds.

1.1. Optimization of the weight ratio of PSBMA hydrogel in mineralized PLGA/PSBMA scaffolds.

The preparation method of PLGA/PSBMA scaffolds with various weight ratio of PSBMA hydrogel was published in our previous study [1]. In this experiment, the weight ratio of PSBMA hydrogel was set as 10 wt%, 20 wt%, 50 wt% and 60 wt%. All PLGA/PSBMA scaffolds were immersed in sterile ultrapure water (pH ~ 8) for 48 h to remove the remnants and stored at -20 °C after freeze drying. Subsequently, the mineralized solution containing with 30 wt% of calcium chloride was prepared and 200 μ L of mineralized solution was dropped on the surface of PLGA/PSBMA scaffolds with various weight ratio of PSBMA hydrogel for 30 min. Then the Ca/P-rich PLGA/PSBMA scaffolds were immersed in ammonium hydroxide (15%, v/v) for 3 h to precipitate calcium phosphate [2]. The mineralized PLGA/PSBMA scaffolds were immersed in sterile ultrapure water (pH ~ 8) for 48 h to remove the remnants and stored at -20 °C after freeze drying. Morphology of surface and cross-section of m-PLGA/PSBMA scaffolds were collected *via* camera.

1.2. Optimization of the volume of mineralized solution.

The PLGA/PSBMA scaffolds with 50 wt% of PSBMA hydrogel and the mineralized solution with Ca^{2+} (3.37 mol/L) were prepared. Then 50 μ L, 100 μ L or 200 μ L of mineralized solution was dropped on the surface of PLGA/PSBMA scaffolds for 30 min. Then the Ca/P-rich PLGA/PSBMA scaffolds were immersed in ammonium hydroxide (15%, v/v) for 3 h to precipitate calcium phosphate. The purification method was referred to the above protocol. The SEM images of surface and cross-section of m-PLGA/PSBMA were measured via SEM.

1.3. Optimization of the concentration of mineralized solution.

The PLGA/PSBMA scaffolds with 50 wt% of PSBMA hydrogel were prepared according aforementioned protocol. The molar concentration of Ca^{2+} in mineralized solution was set at 1.69, 3.37 and 4.21 mol/L, and 200 μ L of mineralized solution was dropped on the surface of PLGA/PSBMA scaffolds for 30 min. Then the Ca/P-rich PLGA/PSBMA scaffolds were immersed in ammonium hydroxide (15%, v/v) for 3 h to precipitate calcium phosphate. The purification method was referred to the above protocol. Morphology of surface and cross-section of mineralized PLGA/PSBMA scaffolds were collected *via* camera..

The weight ratio of PSBMA hydrogel in m-PLGA/PSBMA scaffolds

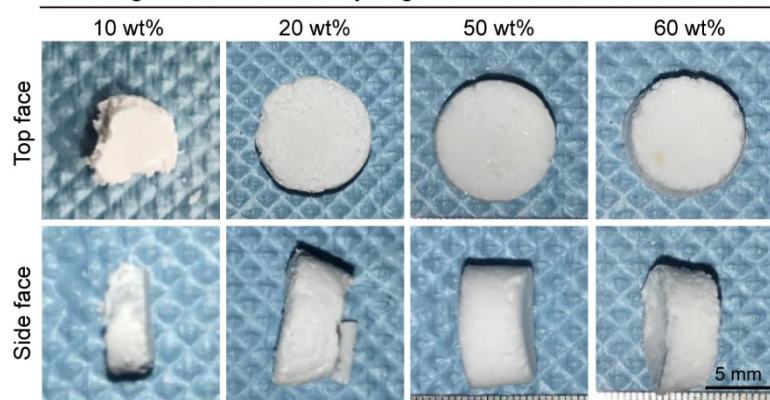


Fig. S1. Morphology of mineralized PLGA/PSBMA scaffolds containing with various weight ratio of PSBMA hydrogel. The mineralized PLGA/PSBMA scaffolds were mineralized in 200 μ L of mineralized solution with Ca^{2+} (3.37 mol/L).

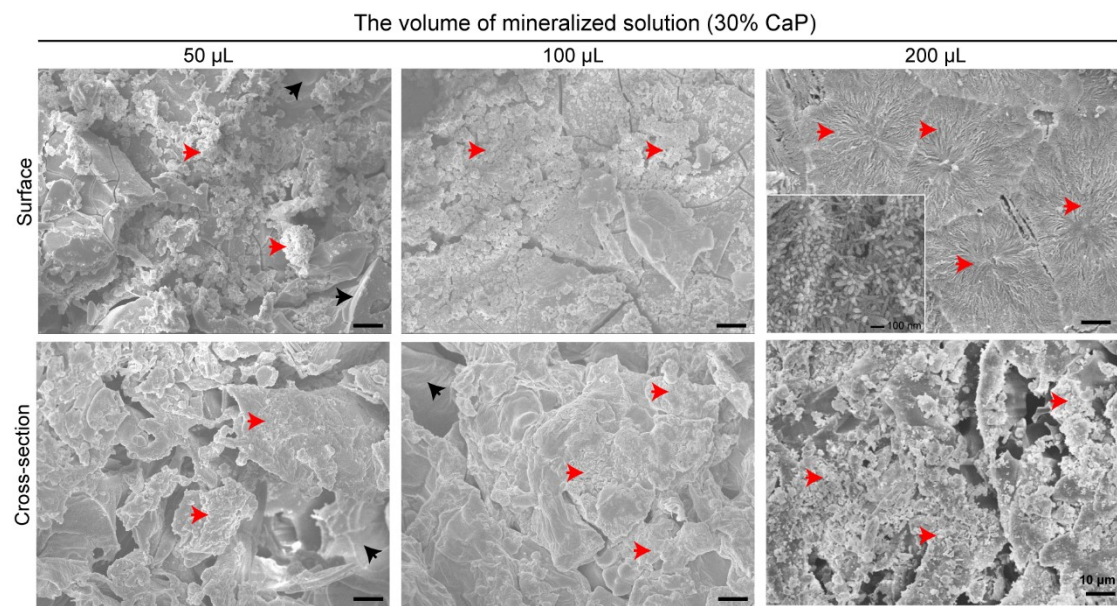


Fig. S2. SEM images of the surface and cross-section of mineralized PLGA/PSBMA. The weight ratio of PSBMA hydrogel was 50 wt%. The molar concentration of Ca^{2+} was served as 3.37 mol/L, and the volume of mineralized solution was set at 50 μ L, 100 μ L or 200 μ L, respectively.

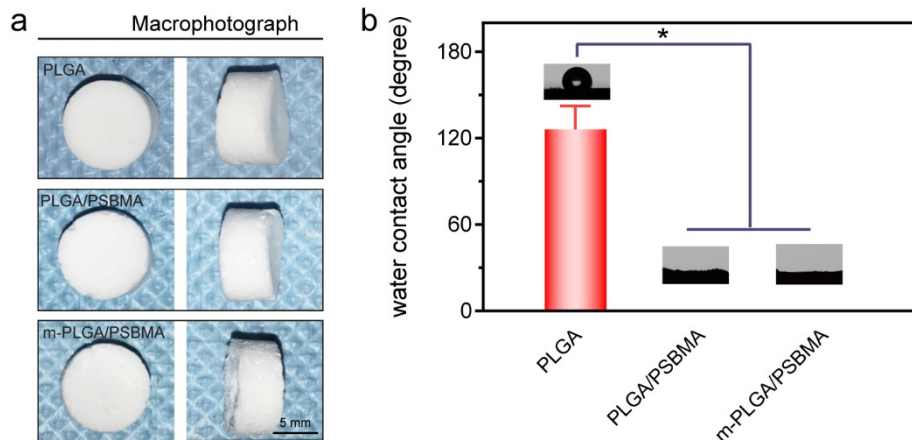


Fig. S3. (a) The representative images of PLGA, PLGA/PSBMA and m-PLGA/PSBMA scaffolds. (b) Images and quantitative analysis of water contact angle of PLGA, PLGA/PSBMA and m-PLGA/PSBMA scaffolds. All data were presented as the mean \pm standard error (SEM) and all differences are significant (* $P < 0.05$, two-way ANOVA) unless denoted as NS (not significant).

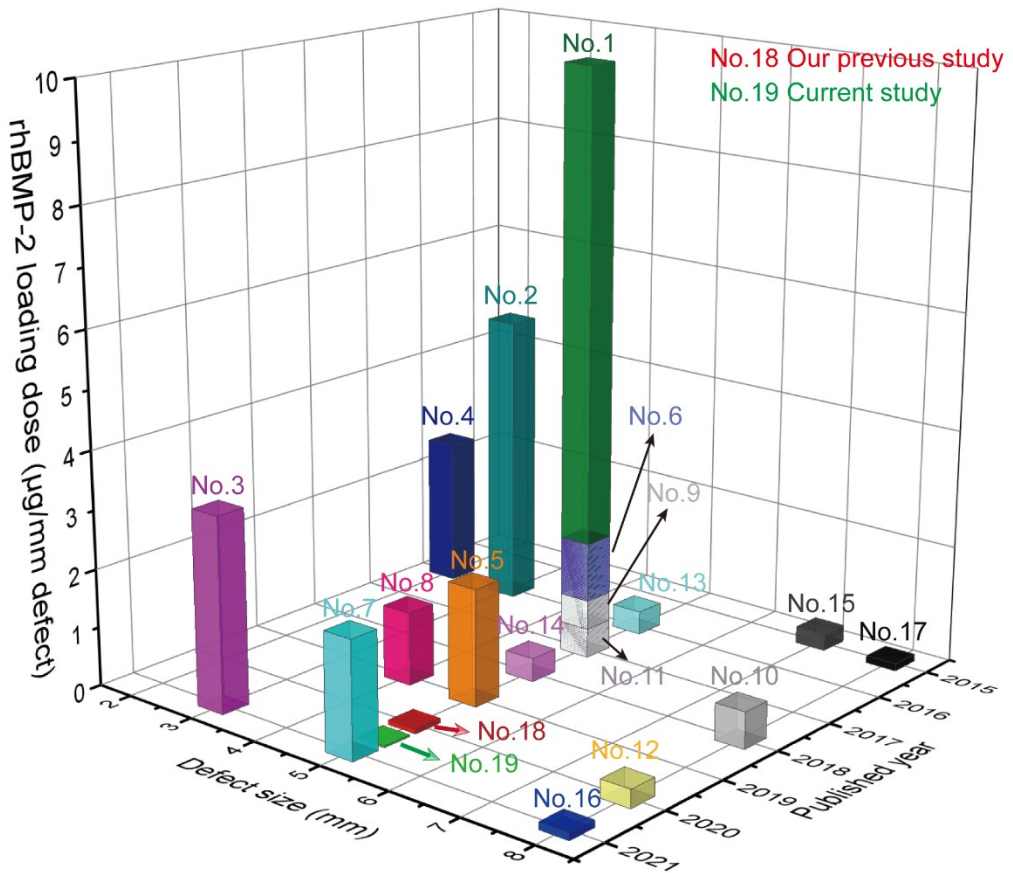


Fig. S4. Summary of rhBMP-2 loading doses on various biodegradable scaffolds for effective healing of critical-sized bone defects in recent five years. The co-delivery of rhBMP-2 with other growth factors, peptides or cells is not included.

Table. S1 Summary of rhBMP-2 loading doses on various biodegradable scaffolds for effective healing of critical-sized bone defects in recent five years. The co-delivery of rhBMP-2 with other growth factors, peptides or cells is not included.

| No. in Fig. 8 | Defected size (mm) | Year | rhBMP-2 loading dose ($\mu\text{g}/\text{mm defect}$) | Ref. |
|---------------|--------------------|------|---|------|
| 1 | 5 | 2017 | 10 | [3] |
| 2 | 3 | 2016 | 5 | [4] |
| 3 | 3 | 2021 | 3.33 | [5] |
| 4 | 2 | 2016 | 2.5 | [6] |
| 5 | 5 | 2019 | 2 | [7] |
| 6 | 5 | 2017 | 2 | [8] |
| 7 | 5 | 2021 | 2 | [9] |
| 8 | 4 | 2019 | 1.25 | [10] |
| 9 | 5 | 2017 | 1 | [11] |
| 10 | 8 | 2018 | 0.625 | [12] |
| 11 | 5 | 2017 | 0.5 | [13] |
| 12 | 8 | 2020 | 0.31 | [14] |
| 13 | 5 | 2016 | 0.4 | [15] |
| 14 | 5 | 2018 | 0.4 | [16] |
| 15 | 7 | 2015 | 0.286 | [17] |
| 16 | 8 | 2021 | 0.125 | [18] |
| 17 | 8 | 2015 | 0.125 | [19] |
| 18 | 5 | 2020 | 0.08 | [1] |
| 19 | 5 | 2020 | 0.03 | * |

* The current study.

References

- [1] P. Liu, L. Sun, Z. Wang, J. Sun, Y. Dong, L. Cao, J. Shen, W.B. Zhang, P. Liu, Biodegradable zwitterion/PLGA scaffold enables robust healing of rat calvarial defects with ultra-low dose of rhBMP-2, *Biomacromolecules* 21(7) (2020) 2844-2855.
- [2] S.H. Jeong, Y.H. Koh, S.W. Kim, J.U. Park, H.E. Kim, J. Song, Strong and Biostable Hyaluronic Acid-Calcium Phosphate Nanocomposite Hydrogel via in Situ Precipitation Process, *Biomacromolecules* 17(3) (2016) 841-51.
- [3] X. Qi, Y. Liu, Z.Y. Ding, J.Q. Cao, J.H. Huang, J.Y. Zhang, W.T. Jia, J. Wang, C.S. Liu, X.L. Li, Synergistic effects of dimethyloxallyl glycine and recombinant human bone morphogenetic protein-2 on repair of critical-sized bone defects in rats, *Sci Rep* 7 (2017) 42820.
- [4] S. Zwingenberger, R. Langanke, C. Vater, G. Lee, E. Niederlohm, M. Sensenschmidt, A. Jacobi, R. Bernhardt, M. Muders, S. Rammelt, S. Knaack, M. Gelinsky, K.P. Gunther, S.B. Goodman, M. Stiehler, The effect of SDF-1 on low dose BMP-2 mediated bone regeneration by release from heparinized mineralized collagen type I matrix scaffolds in a murine critical size bone defect model, *J Biomed Mater Res A* 104(9) (2016) 2126-2134.
- [5] Z. Bal, F. Korkusuz, H. Ishiguro, R. Okada, J. Kushioka, R. Chijimatsu, J. Kodama, D. Tateiwa, Y. Ukon, S. Nakagawa, E.C. Dede, M. Gizer, P. Korkusuz, H. Yoshikawa, T. Kaito, A novel nano-hydroxyapatite/synthetic polymer/bone morphogenetic protein-2 composite for efficient bone regeneration, *Spine J* 21(5) (2021) 865-873.
- [6] S. Bougioukli, A. Jain, O. Sugiyama, B.A. Tinsley, A.H. Tang, M.H. Tan, D.J. Adams, P.J. Kostenuik, J.R. Lieberman, Combination therapy with BMP-2 and a systemic RANKL inhibitor enhances bone healing in a mouse critical-sized femoral defect, *Bone* 84 (2016) 93-103.
- [7] S.H. Han, S.H. Jung, J.H. Lee, Preparation of beta-tricalcium phosphate microsphere-hyaluronic acid-based powder gel composite as a carrier for rhBMP-2 injection and evaluation using long bone segmental defect model, *Journal of Biomaterials Science, Polymer Edition* 30(8) (2019) 679-693.
- [8] Y.H. Ji, M.B. Wang, W.Q. Liu, C.S. Chen, W. Cui, T.F. Sun, Q.L. Feng, X.D. Guo, Chitosan/nHAC/PLGA microsphere vehicle for sustained release of rhBMP-2 and its derived synthetic oligopeptide for bone regeneration, *J Biomed Mater Res A* 105(6) (2017) 1593-1606.
- [9] M. Fenelon, M. Etchebarne, R. Siadous, A. Gremare, M. Durand, L. Sentilhes, S. Catros, F. Gindraux, N. L'Heureux, J.C. Fricain, Comparison of amniotic membrane versus the induced membrane for bone regeneration in long bone segmental defects using calcium phosphate cement loaded with BMP-2, *Mater Sci Eng C Mater Biol Appl* 124 (2021) 112032.
- [10] K. Stuckensen, J.M. Lamo-Espinosa, E. Muñoz-López, P. Ripalda-Cemboráin, T. López-Martínez, E. Iglesias, G. Abizanda, I. Andreu, M. Flandes-Iparraguirre, J. Pons-Villanueva, Anisotropic cryostructured collagen scaffolds for efficient delivery of RhBMP-2 and enhanced bone regeneration, *Materials* 12(19) (2019) 3105.
- [11] B.-B. Seo, J.-T. Koh, S.-C. Song, Tuning physical properties and BMP-2 release rates of injectable hydrogel systems for an optimal bone regeneration effect, *Biomaterials* 122 (2017) 91-104.
- [12] E.B. Bae, K.H. Park, J.H. Shim, H.Y. Chung, J.W. Choi, J.J. Lee, C.H. Kim, H.J. Jeon, S.S. Kang, J.B. Huh, Efficacy of rhBMP-2 Loaded PCL/beta-TCP/bdECM Scaffold Fabricated by 3D Printing Technology on Bone Regeneration, *Biomed Res Int* (2018).
- [13] T. Nakamura, Y. Shirakata, Y. Shinohara, R.J. Miron, K. Hasegawa-Nakamura, M. Fujioka-Kobayashi, K. Noguchi, Comparison of the effects of recombinant human bone morphogenetic protein-

- 2 and-9 on bone formation in rat calvarial critical-size defects, *Clin Oral Invest* 21(9) (2017) 2671-2679.
- [14] S.H. Han, J. Lee, K.M. Lee, Y.Z. Jin, H.-s. Yun, G. Kim, J.H. Lee, Enhanced healing of rat calvarial defects with 3D printed calcium-deficient hydroxyapatite/collagen/bone morphogenetic protein 2 scaffolds, *Journal of the mechanical behavior of biomedical materials* 108 (2020) 103782.
- [15] X.F. Shen, Y.X. Zhang, Y. Gu, Y. Xu, Y. Liu, B. Li, L. Chen, Sequential and sustained release of SDF-1 and BMP-2 from silk fibroin-nanohydroxyapatite scaffold for the enhancement of bone regeneration, *Biomaterials* 106 (2016) 205-216.
- [16] D. Mumcuoglu, S. Fahmy-Garcia, Y. Ridwan, J. Nickel, E. Farrell, S.G.J.M. Kluijtmans, G.J.V.M. van Osch, Injectable Bmp-2 Delivery System Based on Collagen-Derived Microspheres and Alginate Induced Bone Formation in a Time- and Dose-Dependent Manner, *Eur Cells Mater* 35 (2018) 242-254.
- [17] E. Quinlan, E.M. Thompson, A. Matsiko, F.J. O'Brien, A. Loez-Noriega, Long-term controlled delivery of rhBMP-2 from collagen-hydroxyapatite scaffolds for superior bone tissue regeneration, *J Control Release* 207 (2015) 112-119.
- [18] Q. Fan, J. Bai, H. Shan, Z. Fei, H. Chen, J. Xu, Q. Ma, X. Zhou, C. Wang, Implantable blood clot loaded with BMP-2 for regulation of osteoimmunology and enhancement of bone repair, *Bioact Mater* 6(11) (2021) 4014-4026.
- [19] I.G. Kim, M.P. Hwang, P. Du, J. Ko, C.W. Ha, S.H. Do, K. Park, Bioactive cell-derived matrices combined with polymer mesh scaffold for osteogenesis and bone healing, *Biomaterials* 50 (2015) 75-86.